5. H. Schlichting, Boundary Layer Theory, 6th edn., McGraw-Hill, New York (1968).
6. W. Schach, Ing.-Arch., **5**, No. 4, 460-467 (1934).
7. Z. H. Chaudhury, J. Fluid Mech., **20**, Pt. 3, 501-511 (1964).
8. S. Inada and Y. Miyasaka, Bull. JSME, **24**, No. 196, 1803-1810 (1981).

EFFECT OF THE PERFORATION OF THE PIPELINE WALL ON THE VELOCITY OF PROPAGATION OF LONG COMPRESSION WAVES IN A FLUID

N. M. Kuznetsov and E. I. Timofeev

UDC 539.4.015.532.59

A model for predicting the velocity of a weak compression wave propagating over a fluid in a tube with perforated holes is suggested. The fluid is retained in the perforations by surface tension. The wave velocity weakly decreases with an increase in the pressure drop over the wave. Examples of particular predictions are given.

The sound wall and shock wave propagation over the fluid in tubes has specific features which are of interest from both theoretical and practical points of view. The speed of sound in such systems can be fairly different from the case of an infinite medium. The dependence of the shock wave speed on the pressure can be also quite peculiar.

The speed of sound C for fluids in tubes has been calculated by N. E. Zhukovskii [1] and is defined by the equation

$$C^2 = \frac{C_f^2}{1 + 2r_0\rho_0 C_f^2/lE}, \tag{1}$$

where E is the Young modulus for the material of tube walls; r_0 and ℓ are the radius of the tube and the thickness of its walls, respectively (it is assumed that $l \ll r_0$).

We next consider sound waves and finite-amplitude waves in the fluid that occupy the tube with perforated walls. It is assumed that the fluid does not wet an external surface of the tube. All perforations are of the same size (diameter A), and on the average, are uniformly distributed over the tube surface. It is assumed that the tube is of an infinite length, and that the wave length is much larger than other linear sizes in the problem [the tube diameter and average distance (A + B) between the perforations]. At the same time, the period when the fluid is present in the wave is large in comparison with the time of establishing a static condition of the fluid in perforation holes. Capillary forces prevent the fluid from effluxing out of the holes. The maximum increment in pressure P^* in the wave at which the capillary forces still retain the fluid in the holes (see Fig. 1) is equal to $P^* = 4\sigma/A$. The gravity is not taken into account. This is admissible in the case of a tube in a horizontal position in the gravity field and when the inequality $\sigma >> \rho_0 g A r_0$ holds.

A plane weak shock wave of infinite length propagating over the fluid in the tube (with no allowance for the friction against the walls) is completely determined by the equations of conservation of mass, momentum, and isentropic compression of a fluid

$$\rho_0 U_0 (S_0 + S_A) = \rho_1 U_1 (S_0 + \Delta S_0) + \rho_1 U_0 S_A; \tag{2}$$

$$(P_0 + \rho_0 U_0^2)(S_0 + S_A) = (P_1 + \rho_1 U_1^2)(S_0 + \Delta S_0) + (P_1 + \rho_1 U_0^2)(S_A + S_h); \tag{3}$$

$$P = P(\rho),\ P = P_1 - P_0,\ \rho = \rho_1 - \rho_0, \tag{4}$$

N. N. Semenov Moscow Institute of Chemical Physics of the Russian Academy of Sciences. Translated from Inzhenerno-fizicheskii Zhurnal, Vol. 64, No. 1, pp. 46-49, January, 1993. Original article submitted December 9, 1991.

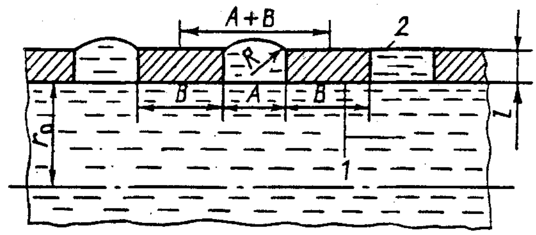

Fig. 1. The scheme of the perforated pipeline: 1) compression wave front, 2) undisturbed liquid surface; A, capillary diameter; B, mean distance between the capillaries; r_0, pipeline radius; l, wall thickness; R, radius of curvature of the disturbed liquid surface. The arrow indicates the direction of the wave motion.

where P_i, ρ_i, and U_i are the pressure, density, and velocity of the liquid in the coordinate system of the shock wave front (subscripts i = 0 and i = 1 correspond to the regions prior to and beyond the front); S_0 and $S_0 + \Delta S_0$ are the area of the transverse cross section of the tube at the pressures P_0 and P_1

$$\Delta S_0 = 2\pi r_0 \Delta r_0;\ \Delta r_0 = \frac{P r_0^2}{l E'}. \tag{5}$$

Here, E′ is the efficient value of the Young modulus for a perforated tube, connected with the Young modulus E for a solid material by the relation $E' = (1 - \pi n A^2/4)E$, where n is the average number of holes per unit of the tube surface; S_A and S_h stand for the additional constituents of the area of the "tube" transverse cross section, associated, respectively, with the volume of the holes and with the fluid emergence outside the outer radius of the tube (Fig. 1). For long waves we cannot take into account the discreteness of hole distribution, and can introduce the averaged efficient values of S_A and S_h

$$S_A = 2\pi r_0 n V_A = \frac{\pi^2 A^2 r_0 l}{2(A+B)^2},\quad S_h = 2\pi r_0 n V_h = \frac{2\pi r_0 V_h}{(A+B)^2}, \tag{6}$$

$$V_h = \Pi h^2 (R - h/3),\ h = R - [R^2 - (A/2)^2]^{1/2},\ R = 2\sigma/P \tag{7}$$

[V_h is the volume of the spherical segment of radius R (see Fig. 1)].

Owing to the restriction $P < P^*$ for macroscopic holes, all terms nonlinear with respect to P in (2)-(4), excluding the term S_h, are negligibly small. Here the dependences of the tube radius and fluid density on the increment in pressure are implied. The first one is defined by the linear approximation (5), and the second follows from (4) and is presented in the form $P = C_f^2 \rho$. The following expressions for U_0 here can be found from (2) and (3)

$$U_0^2 = \frac{1 + \bar{S}_A + P_0(\Delta\bar{S}_0 + \bar{S}_h)/P}{(1 - \bar{S}_A)/C_f^2 + \rho_0(\Delta\bar{S}_0 + \bar{S}_h)/P}. \tag{8}$$

For $P \ll P^*$ the equality $P \gg h$ holds and from (6) and (7) it follows

$$V_h = \frac{\pi A^4 P}{128\sigma},\ \bar{S}_h = \frac{\pi A^4 P}{64\sigma r_0 (A+B)^2},$$
$$\Delta\bar{S}_0 = \Delta S_0/S_0,\ \bar{S}_A = S_A/S_0,\ \bar{S}_h = S_h/S_0. \tag{9}$$

In a wide range of parameters Eq. (8) assumes the following further simplifications:

1) assuming that the total area of the holes is at least not larger than the rest surface of the tube, from (6) we obtain $\bar{S}_A \ll 1$;

2) the value of $P_0 \Delta S_0/P$ for a not very thin-wall tube (for example, for $\ell/r_0 > 10^{-3}$) is much less than unity, since when $P_0 \approx 1$ atm, the ratio E/P for metals is very high;

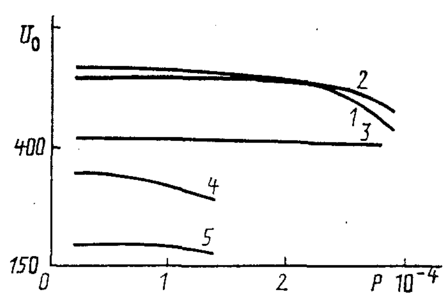

Fig. 2

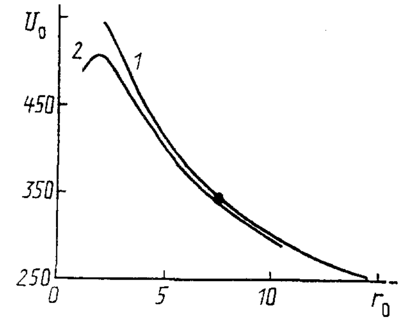

Fig. 3

Fig. 2. Dependence of the compression wave velocity on the pressure drop at the wave front: curves 1, 2, 3 are constructed at $A = B = 10^{-5}$ m, $\ell = 10^{-4}$ m, $r_0 = 1, 2, 3$ cm; 4, 5) for $A = 2 \cdot 10^{-5}$ m, $B = 10^{-5}$ m and $l = 10^{-4}$ and 10^{-5} m; $E' = 2 \cdot 10^{11}$ N/m^2. U_0 m/sec; P, Pa.

Fig. 3. Dependence of the compression wave velocity on the pipeline radius: curves 1 and 2 correspond to the pressures $P = 10^3$ and 2.7×10^4 Pa; $A = B = 10^{-5}$ m, $E' = 2 \cdot 10^{11}$ N/m^2, $l = 10^{-4}$ m. r_0, cm.

3) the second term in the numerator of (8), as can be easily verified, is also small as compared to unity within the wide range of the values of σ and A (for example, at $\sigma = 0.073$ N/m, the factor of surface tension of water at the temperature 20°C and $A < 1$ cm).

Having satisfied all of the three indicated inequalities, instead of (8) we write down

$$U_0^2 = \frac{C_f^2}{1 + \rho_0 C_f^2 \left(\frac{2r_0}{E'l} + \frac{\bar{S}_h}{P} \right)}. \tag{10}$$

For $P \ll P^*$ the speed U_0, according to (9) and (10), does not depend on P and can be put in the form

$$U_0^2 = \frac{C_f^2}{1 + \rho_0 C_f^2 \left[\frac{2r_0}{E'l} + \frac{\pi A^3}{16 P^* r_0 (A+B)^2} \right]}. \tag{11}$$

This exactly is the speed of sound in the original system under consideration. In the case of a solid tube, i.e. at $A = 0$, Eq. (11) coincides with (1).

In the case of finite intensities of the wave, its rate decreases with an increase in P. This follows from a nonlinear positive dependence of the volume V_h on the pressure: $d(V_h/P)/dP > 0$. The dependence of U_0 on P and r_0 for water is shown in Figs. 2 and 3. In systems with such a dependence of U_0 on P, there are isentropic compression waves of finite amplitude and shock expansion waves (in their motion, expansion waves are compressed, thus converting to shock compression waves, whereas compression waves are expanded). However, a relative decrease in the speed U_0 with the pressure P (for the values of the parameters of the same order as in the case presented in Fig. 2) is very small and it leads to significant deformation of waves only when they pass over the distances, large enough so that viscosity effects can be significant.

Based on the calculations performed, one can draw the following conclusions. The presence of perforation holes in the tube wall leads to a decrease in the speed of the propagation of weak disturbances over the fluid occupying the tube, as compared to the case of an infinite fluid and the case considered in [1]. It can be useful to know the value of U_0 in predicting hydrodynamic processes, for example in systems of transpirational cooling.

NOTATION

C_f, speed of sound in an infinite fluid; A, hole diameter; C, speed of sound; B, distance between the holes; P, pressure drop at the compression wave; σ, surface tension coefficient; g, acceleration of gravity; P_0 and P_1, pressure ahead of the compression wave and beyond its front; ρ_0 and ρ_1, fluid density ahead of the compression wave and beyond its front; U_0 and U_1, fluid velocities in the coordinate system of the compression wave front; S_0, initial area of the tube; ΔS_0, increment in area.

REFERENCES

1. N. E. Zhukovskii, Collected Works, Vol. 3 [in Russian], Moscow–Leningrad (1949).

DIELECTRIC VISUALIZATION OF THE CONVECTIVE INSTABILITY IN NONPOLAR NONVISCOUS FLUIDS

A. A. Potapov

UDC 532.517:537.226

The dielectric method is used to study the convective instability in nonpolar nonviscous fluids "heated from below" at different temperature gradients (0.1-0.005 K/cm). Different types of resonant cavities are used as measuring cells; their specific feature is the pronounced nonuniformity of the electromagnetic field which has become a decisive factor in convective flow detection.

Heat convection in a heated fluid layer is the simplest case of hydrodynamic instability and, at the same time, is a striking example of how a system disturbed from a thermodynamic equilibrium state can change to a highly ordered state. In hydrodynamics, convective instability is "one of the most curious and difficult problems of classical physics" [1]. Benard's effect is the most striking example of the convective instability. It manifests itself in forming a regular cellular structure of the fluid heated from below under certain conditions. As these processes are fundamental in nature, Benard's convection has become the subject of many theoretical and experimental studies.

At present the experimental methods of studying convective flows have attained certain success. The traditional methods (such as hot-wire, photo visualization, acoustic, interferometric) continue to improve. The high effective laser Doppler method of measuring spatial and time parameters of flows [1-5] has been developed.

The measured parameters of natural convection are small in magnitude and require special recording facilities. Great difficulties spring up when determining the spatial-time temperature, pressure, and velocity fields of a test medium in closed volumes. Hence, further improvement of the visualization methods of convective flows remains urgent and expedient.

The ability to investigate hydrodynamic processes by the dielectric method is based on the close relationship between the dielectric properties of the substance and its molecular density [6]. The matter equations of electrodynamics contain the dielectric permeability (DP) which refers to the specific characteristics of the substance and depends on the mass density and, hence, on the flow and heat transfer parameters of this substance. In a more general form, this relationship may be given as [6]

$$F(\varepsilon) = \frac{4\pi\alpha\rho}{\mu}, \tag{1}$$

where F(ε) is the dielectric function representing some structure composed of static ε_s and quasioptic ε_∞ dielectric permeabilities and the number coefficients; α is the polarizability of molecules; μ is the molar mass; ρ is the substance density.

Automation and Engineering Physics Department of the Irkutsk Research Center, Russian Academy of Sciences, Irkutsk, Russia.

Translated from Inzhenerno-fizicheskii Zhurnal, Vol. 64, No. 1, pp. 50-57, January, 1993. Original article submitted April 19, 1991.

1062-0125/93/6401-0040$12.50